The Monsoon Rainband over China and Relationships with the Eurasian Circulation

ARTHUR N. SAMEL, WEI-CHYUNG WANG, AND XIN-ZHONG LIANG

Atmospheric Sciences Research Center, The University at Albany, State University of New York, Albany, New York

(Manuscript received 13 November 1996, in final form 30 January 1998)

ABSTRACT

Yearly variations in the observed initial and final dates of heavy, persistent monsoon rainband precipitation across China are quantified. The development of a semiobjective analysis that identifies these values also makes it possible to calculate annual rainband duration and total rainfall. Relationships between total rainband precipitation and the Eurasian circulation are then determined. This research is designed such that observed rainband characteristics can be used in future investigations to evaluate GCM simulations.

Normalized daily precipitation time series are analyzed between 1951 and 1990 for 85 observation stations to develop criteria that describe general rainband characteristics throughout China. Rainfall is defined to be ''heavy'' if the daily value at a given location is greater than 1.5% of the annual mean total. Heavy precipitation is then shown to be ''persistent'' and is thus identified with the rainband when the 1.5% threshold is exceeded at least 6 times in a 25-day period. Finally, rainband initial (final) dates are defined to immediately follow (precede) a minimum period of 5 consecutive days with no measurable precipitation. A semiobjective analysis based on the above definitions and rainband climatology is then applied to the time series to determine annual initial and final dates.

Analysis application produces results that closely correspond to the systematic pattern observed across China, where the rainband arrives in the south during May, advances to the Yangtze River valley in June, and then to the north in July. Rainband duration (i.e., final − initial + 1) is approximately 30–40 days while total rainfall decreases from south to north. A significant positive correlation is found between total rainfall and duration interannual variability, where increased rainband precipitation corresponds to initial (final) dates that are anomalously early (late). No clear trends are identified except over north China, where both duration and total rainfall decrease substantially after 1967.

The Eurasian sea level pressure and 500-hPa height fields are then correlated with total rainfall over south China, the Yangtze River valley, and north China to identify statistically significant relationships. Results indicate that precipitation amount is influenced by the interaction of several circulation features. Total rainfall increases over south China when the surface Siberian high ridges to the south and is overrun by warm moist air aloft. Yangtze River valley precipitation intensifies when westward expansion of the subtropical high along with strengthening of the Siberian high and monsoon low cause moisture advection, upward motion, and the thermal gradient along the Mei-Yu front to increase. North China total rainfall increases in response to intense heating over the landmass, westward ridging of the subtropical high, and greater moisture transport over the region.

1. Introduction

The climate of China is strongly influenced by the east Asian monsoon. The primary physical manifestation of the summer monsoon is persistent, heavy precipitation identified with a coherent, well-defined rainband. In general terms, rainband movement is characterized by a stepwise poleward advance from south China to the Yangtze River valley to north China (Ding 1992, 1994; Tao and Chen 1987; Lau and Li 1984; Lau et al. 1988; Lau and Yang 1996). Embedded within the rainband are mesoscale convective features that can produce locally heavy precipitation (Chang and Chen 1995; Ding 1992, 1994; Ninomiya and Akiyama 1992). During the period when a region is affected by the rainband, precipitation is typically interrupted by several ''break periods'' when little or no rain occurs. Break period length varies from a few days to approximately two weeks. Total rainband precipitation is greatest over south China and decreases to the north, where the mean pattern is determined by the configuration of the Eurasian circulation (Samel et al. 1995; Chen and Chen 1995).

While the average rainband structure over east Asia is well known, precipitation undergoes substantial interannual variability. These variations have an extremely important impact on the economy of China (Hulme et al. 1994), where agricultural production is highly dependent upon the monsoon. Two different approaches have been used in previous studies to quantify rainband

Corresponding author address: Dr. Arthur N. Samel, Department of Geography, Bowling Green University, Hanna Hall, Bowling Green, OH 43403-0217.
E-mail: ansamel@bgnet.bgsu.edu

interannual variability. First, annual variations in the initial and final dates of heavy, persistent precipitation are determined following a subjective data analysis (e.g., Tao and Chen 1987; Liu et al. 1994). While this isolates the rainband period, it lacks sufficient rigor to ensure that a consistent set of criteria are used to identify the rainband. Second, precipitation is assumed to occur during a prescribed period of several months (Huang and Wang 1985; Lau et al. 1988; Samel et al. 1995; Liang et al. 1994; Nitta and Hu 1996). The imposition of an artificial rainband period, however, reflects an inability to objectively quantify yearly variations in the initial and final dates of heavy, persistent rainfall across China.

Although rainband duration at a given location is typically on the order of one month (Tao and Chen 1987), the monsoon can be active as early (late) as April (September) (Lau et al. 1988; Ding 1992, 1994). Thus, while the choice of an unrealistically long period ensures that the monsoon rainband is considered in any subsequent analysis, it also allows for additional sources of heavy precipitation (e.g., extratropical disturbances in north China and tropical activity over the south) to be erroneously attributed to the rainband. This, in turn, makes it more difficult to identify physically intuitive relationships between rainband and Eurasian circulation interannual variability due to the mixing of atmospheric mechanisms that have subseasonal temporal variations.

In spite of the problems identified with the use of subjective analyses and invariant monsoon periods, a large number of studies have investigated associations that exist between summer precipitation over China and Eurasian circulation variations. Tao and Chen (1987) found that the poleward extent of the rainband increases as the subtropical high over the west-central Pacific Ocean moves farther to the north. Huang and Wang (1985) showed that the region with the heaviest summer rainfall is related to the westward expansion of the subtropical high, where precipitation increases to the north as the high ridges farther to the west. Similar relationships were identified by Yatagai and Yasunari (1994, 1995), Fan and Oglesby (1996), and Nitta and Hu (1996). Lau et al. (1988) indicated that the stepwise poleward advance of the monsoon rainband over east Asia can be explained by interactions between the Eurasian circulation and eastward-propagating 40–50-day waves (Madden and Julian 1972).

Both Samel et al. (1995) and Liang et al. (1994) concluded that summer rainfall interannual variability over east China is influenced by the interaction of several Eurasian circulation features. At the surface, these include the monsoon low over south-central Asia, the subtropical high over the west-central Pacific Ocean, the Mei-Yu front along the Yangtze River valley, and the Siberian high over south-central Siberia (Fig. 1a). The 500-hPa-height pattern (Fig. 1b) clearly reveals the baroclinic nature of the monsoon low (i.e., upper-level monsoon high) and barotropic reflection of the subtropical high while both the Mei-Yu front and Siberian high are identified as shallow features.

Several general circulation model (GCM) investigations have analyzed the ability of numerical models to simulate observed east Asian summer rainfall characteristics when the monsoon is assumed to have an invariant period. Samel et al. (1995) showed that GCM-generated centers of anomaly interannual variability over north China, the Yangtze River valley, and south China are similar to observations. Liang et al. (1994) identified large decadal variations over the same regions. Sperber et al. (1994) found that the simulated poleward advance of rainfall over China during June and July became more detailed and realistic as the horizontal grid resolution was increased. Liu et al. (1994) indicated that the stepwise progression of the monsoon rainband during 1990 was reproduced when a high resolution regional mesoscale model grid was inserted into a GCM over east Asia and adjacent ocean regions. Fan and Oglesby (1996) determined that total summer precipitation over north China is strongly related to the position of subtropical high.

While the research cited above indicates that GCMs can reproduce fundamental features of the summer rainfall field over east Asia, the objective identification of simulated monsoon rainband initial and final dates has not been investigated, nor have relationships between GCM rainband and Eurasian circulation interannual variability. This has been precluded by the current inability to quantify observations. Hence, this study has two goals. The first is to determine observed monsoon rainband interannual variability in China. To accomplish this, a semiobjective analysis is developed and applied to daily rainfall station data to identify annual rainband initial and final dates. The resulting values are then used to calculate rainband duration and total rainfall. The second goal is to identify relationships between these rainband characteristics and circulation features in the Eurasian sea level pressure and 500-hPa height fields. This study is designed such that the observed monsoon rainband characteristics can be used in future investigations to evaluate GCM simulations.

A description of the data used in this study is given in section 2. In addition, the specific criteria used to determine annual initial and final rainband dates throughout China are developed in section 2. The application of these criteria is discussed in section 3. Yearly variations in rainband initial and final dates, duration, and total precipitation are analyzed in section 4. Relationships between total rainband precipitation and Eurasian circulation interannual variability are determined in section 5. The results of this study are summarized and future research topics discussed in section 6.

2. Data and monsoon rainband identification

East Asian summer monsoon rainband characteristics are investigated for the period 1951–90. This time frame

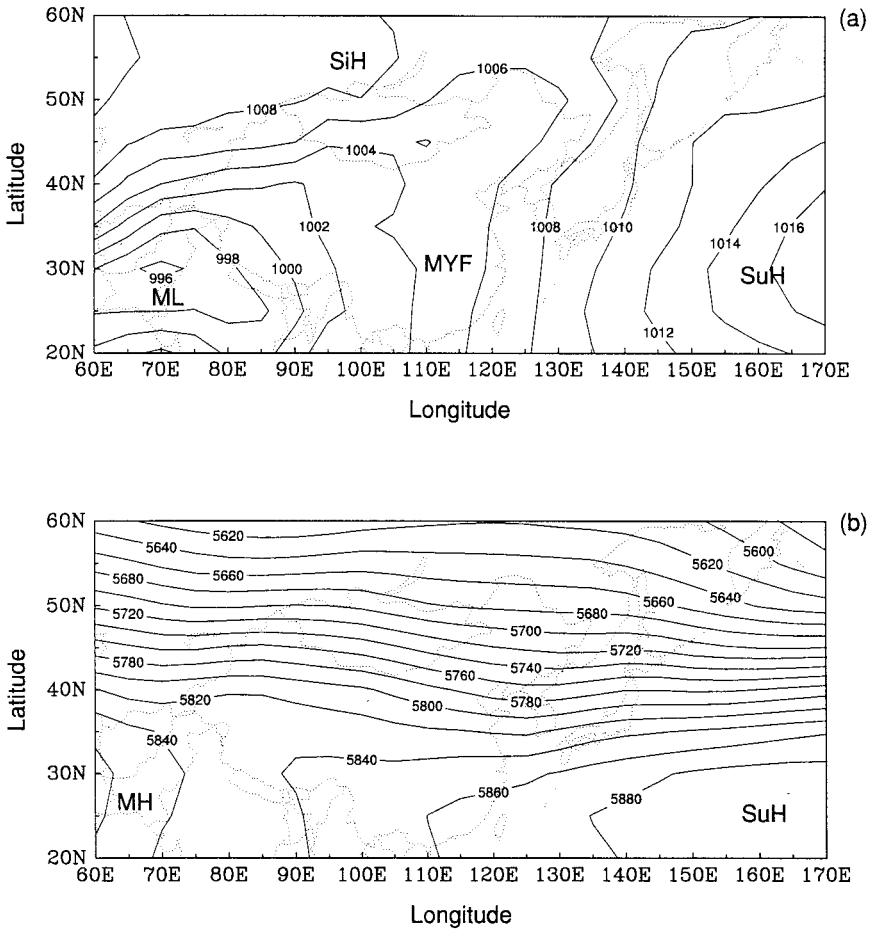

FIG. 1. (a) Mean June, July, August sea level pressure and (b) 500-hPa-height fields over Eurasia for the period 1951–90. Surface circulation features are the monsoon low (ML), subtropical high (SuH), Siberian high (SiH), and Mei-Yu front (MYF), where the contour interval is 2 mb. The 500-hPa features include the subtropical high (SuH) and monsoon high (MH), where the contour interval is 20 m.

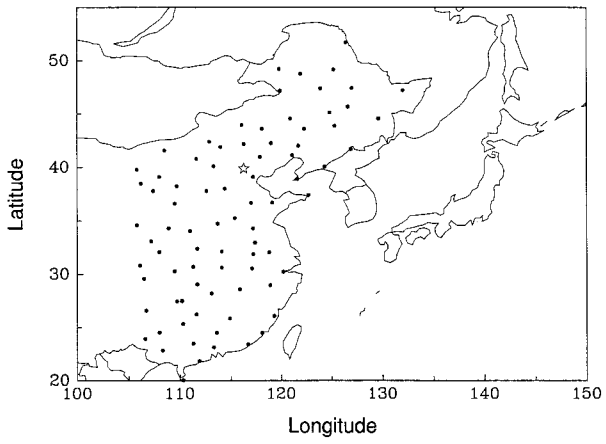

FIG. 2. Locations of the 85 observation stations where 1951–90 daily precipitation data are analyzed. Values at Beijing (star) are discussed in greater detail in section 3.

is chosen because data coverage in China prior to 1951 is relatively sparse while the quality of more recent values has not been determined. In this study, daily precipitation data for 85 stations (Fig. 2; Tao et al. 1991) are used to examine initial and final rainband dates, duration, and total rainfall (also referred to as total rainband precipitation). These stations are uniformly distributed over east China and are chosen because they contain virtually no data discontinuities. The precipitation records begin in January 1951 for 60 stations and prior to 1955 at the remaining locations. Data for all stations extend through December 1990. Precipitation at each location is normalized by the mean annual total for that station such that daily values are given as a percentage of the annual mean. This normalization eliminates geographical differences in annual average amount such that the value at all locations becomes 1.00. This aids in the development and application of uniform criteria to identify monsoon rainband characteristics and is discussed below.

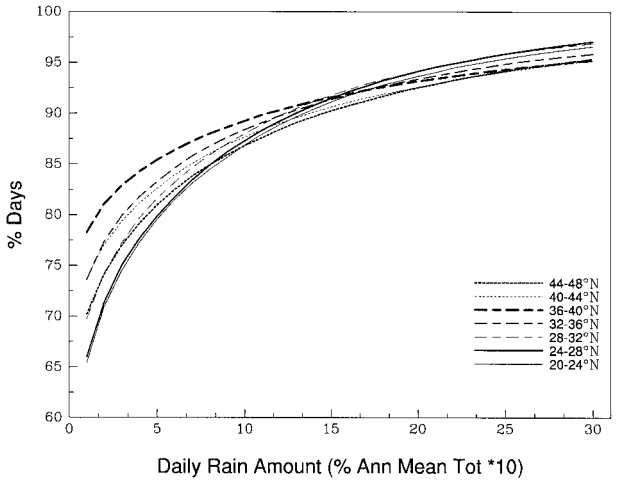

FIG. 3. Cumulative frequency distributions (CFDs) of the percentage of days (ordinate) as a function of daily rainfall amount (% annual mean total) times 10. Each CFD represents values for a 4° zonal band (see legend), where daily time series for the stations in each band are analyzed between April and September.

Monthly sea level pressure and 500-hPa height anomaly data for the period January 1951–December 1990 are provided for a 5° latitude × 5° longitude grid that extends from 20° to 90°N and 180°E to 180°W (Jenne 1989). These data will be used in section 4 to ascertain statistically significant relationships between monsoon rainband characteristics and Eurasian circulation features.

Given that the summer monsoon rainband is a coherent physical feature associated with the occurrence of heavy, persistent precipitation, it follows that there exists at least one set of conditions that can be used to identify the initial and final dates of rainband precipitation throughout China. The remainder of this section focuses on the development of criteria for heavy rainfall, persistent rainfall, and the consecutive number of rain free days that signal rainband initiation and withdrawal.

The daily precipitation data are first analyzed to establish the value that must be exceeded to define rainfall for a given day as ''heavy.'' Cumulative frequency distributions (CFDs) of daily amount are generated for 4° latitude bands (i.e., 20°–24°N, 24°–28°N, . . . , 44°–48°N) across China and shown in Fig. 3. Each CFD is based on the stations located within that zonal band and represents a composite of all days between April and September for the period 1951–90. The April through September time frame is chosen because it marks the period during which the rainband is active over China. The analysis of precipitation over latitudinal bands is based on observed rainband zonal alignment and the use of a similar procedure by Liang et al. (1994) to assess summer rainfall interannual variability. Figure 3 shows that the CFDs become skewed toward lower amounts as latitude increases and indicates a decrease in the total number of rainfall days to the north as the

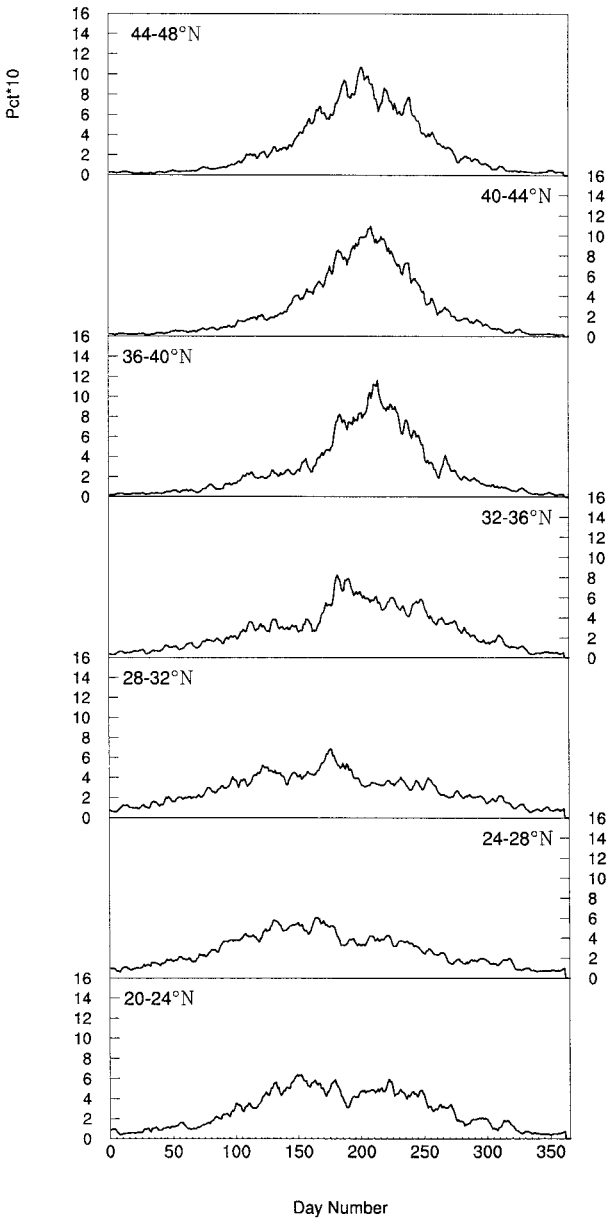

FIG. 4. Mean daily precipitation profiles over the period 1951–90 for 4° zonal bands (20°–24°N, 24°–28°N, . . . , 44°–48°N) across China. Day numbers (31 December = day 365) are given along the abscissa while precipitation (percentage of the annual mean total times 10) is listed along the ordinate.

rainband becomes the primary precipitation source for these bands. The exception occurs over the north, where additional rainfall is attributed to the passage of extratropical disturbances (Tao and Chen 1987). These results are borne out by Fig. 4, which shows the 1951–90 mean daily precipitation profiles across China. The 20°–24°N plot reveals two distinct maxima, where the first is identified with the rainband and the second with tropical activity following rainband passage (Ding 1994). As latitude increases, the tropical signal fades and a single

dominant peak identified with the rainband is established. Peak amplitude, which indicates rainband contribution to annual total precipitation, decreases north of 40°N and underscores the increased contribution of midlatitude systems. In spite of these regional differences, Fig. 3 shows that, for each band, precipitation values during approximately 90% of the days are less than 1.5% of the annual mean. The 90% value is used as an approximate statistical threshold, where amounts that exceed this threshold are considered to be significantly greater than zero. Thus, for each station, rainfall is defined to be heavy when the daily amount exceeds 1.5% of the annual average for that location. Note that the daily rainfall values in Fig. 4 represent a 1951–90 composite for all stations located in each zonal band. As a result, amounts are much less than the 1.5% threshold just identified.

We then expand the heavy rainfall definition to include ''persistence,'' which is defined as the minimum number of days during a specified time interval when rainfall exceeds 1.5%. This time span must be sufficiently large to ensure that precipitation breaks during the rainband period are not mistakenly identified with initiation or withdrawal. Thus, the interval over which persistence is defined will first be determined. For a given station and year, the daily precipitation time series is analyzed between the initial and final exceedences of the 1.5% threshold to determine the number of days that separate adjacent heavy rainfall days. Then, as above, composites of these period lengths are used to produce CFDs for the zonal bands. Results (Fig. 5a) reveal that the CFDs become skewed toward shorter period lengths with increasing latitude. Given the substantial rainband contribution to total annual precipitation in the northern zones (i.e., Fig. 4), an increasing number of days during the rainband period have amounts that exceed 1.5% and, as a result, the intervals that separate these days decrease. Regardless of this zonal variation, the 90% threshold is exceeded by all bands at approximately 25 days and this time span is chosen as the period over which the persistence definition is developed.

To establish the minimum number of days during a 25-day period when rainfall must exceed 1.5% of the annual mean total, a 25-day ''moving window'' is applied to the annual time series for each station in that band. For a given location and year, the initial 25-day period is placed such that the first day corresponds to the first 1.5% exceedence in the time series. The total number of days during this period when rainfall exceeds 1.5% is calculated. The first and last days of the 25-day period are then moved forward one day in time and the total number of 1.5% exceedences is again determined. This iterative process continues until the last day of the 25-day window coincides with the final 1.5% exceedence in the annual time series. When the analysis has been completed for all stations in the band, a composite of the number of heavy rainfall days for all 25-day windows is used to develop the corresponding CFD.

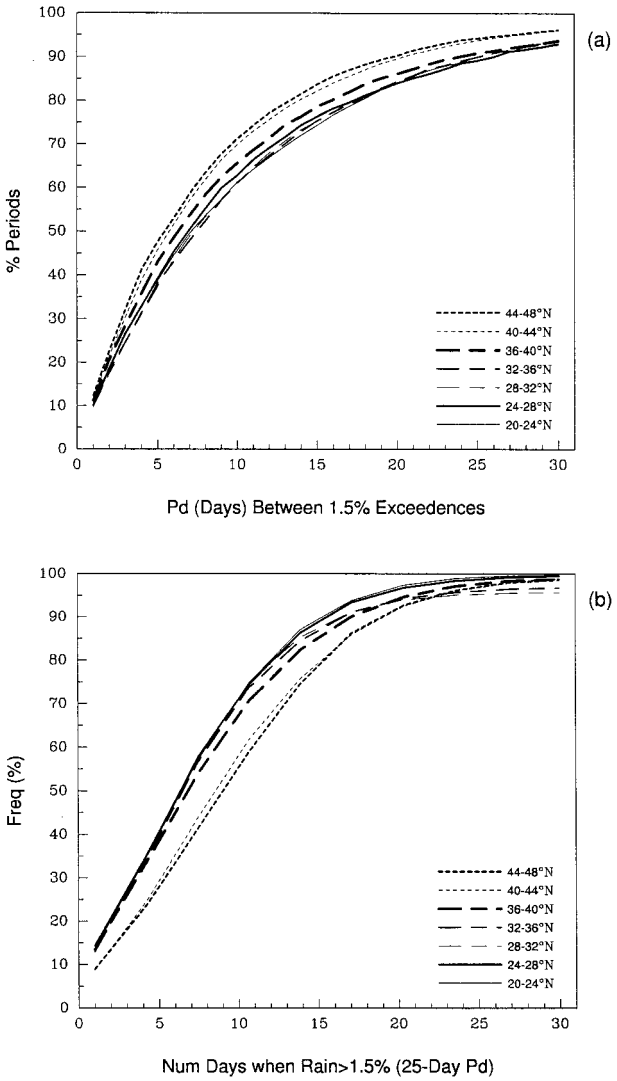

FIG. 5. CFDs of (a) the percentage of periods (ordinate) as a function of period length, in days, between 1.5% exceedences (abscissa), and (b) the percentage of 25-day periods as a function of the number of days in a 25-day period when precipitation exceeds 1.5%. The yearly precipitation time series for stations in each 4° zonal band are analyzed between the first and last days when values are greater than 1.5%.

The results for all bands are shown in Fig. 5b and show that the CFDs become skewed toward higher values as latitude increases. This is explained by the relatively large number of days in the northern zones when rainfall amounts exceed 1.5%. In spite of this zonal variation, roughly 90% of the 25-day windows have six or less exceedences. On the basis of this result, precipitation throughout China is defined to be both heavy and persistent when daily rainfall exceeds 1.5% of the annual mean at least six times in a 25-day period. Hereafter, the occurrence of heavy persistent precipitation will be identified with the monsoon rainband. Given that the rainband period at a specific location is marked by the

initiation and withdrawal of persistent rainfall, the 25-day running window will be an important component of the analysis developed in section 3 to quantify initial and final dates.

Finally, the intensity of the hydrologic cycle over China is assessed to determine the minimum length of the rain free period that immediately precedes (follows) rainband initiation (withdrawal). To facilitate this analysis, the duration of a single rain event is specified to be the consecutive number of days during which precipitation is measured. Conversely, the length of a dry period is defined as the consecutive number of days with zero rainfall.

For all locations within a specific zonal band, 25-day running windows are applied to the time series between April and September to identify and aggregate windows into groups based on persistent and nonpersistent precipitation. For both sets of windows, rain event lengths are calculated and frequency distributions based on these values are generated. Figure 6a shows the distributions constructed with windows where rainfall is not persistent. Results indicate that the distributions are skewed toward lower values as latitude increases and correspond to a decrease in the number of days with measurable precipitation to the north. The exception is north of 40°N where midlatitude disturbances contribute additional precipitation. Nevertheless, at least 90% of the rainfall events are less than or equal to 5 days in duration. Frequency distributions for the persistent rainfall windows (not shown) have the same zonal tendency although, relative to the nonpersistent windows, values are skewed to the right due to an increase in the number of rainfall days. These results indicate that the hydrologic cycle is rarely active over a period that exceeds 5 days during windows not identified with the rainband.

The procedure just described is then repeated, where the pooled windows are now analyzed to develop dry period frequency distributions. The results for windows with persistent rainfall (Fig. 6b) indicate that the distributions are skewed toward larger values with increasing latitude. This occurs because the number of rain-free days increases with latitude. The exception is again found over the northern zones. At least 90% of the dry periods in each zonal band are less than or equal to 5 days in length. Frequency distributions for the nonpersistent windows (not shown) have the same zonal signal while period lengths become more skewed to the right as the number of rain-free days increases. These results show that the hydrologic cycle is rarely dormant more than 5 successive days during persistent rainfall periods. Thus, for a specific location and year, a minimum period of 5 consecutive days with no measurable precipitation is required to identify monsoon rainband initiation and withdrawal. Note that this period length also corresponds to typical break period duration. We will elaborate on the application of a minimum 5-day dry period to identify initial and final rainband dates in the following section.

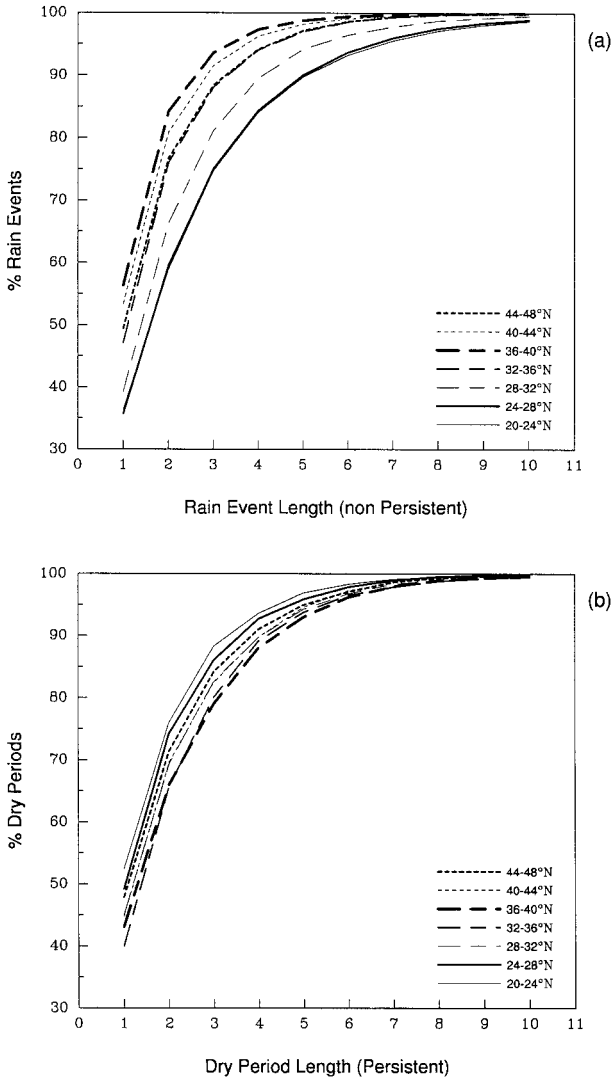

FIG. 6. CFDs of (a) the percentage of rain events (ordinate) as a function of rain event length for all 25-day windows with nonpersistent rainfall (abscissa), and (b) the percentage of dry periods as a function of dry period length for all 25-day windows with persistent rainfall. The yearly time series are analyzed between April and September.

3. Identification of initial and final rainfall dates

The poleward march of the monsoon rainband across China has a well-defined seasonal signal. Thus, for a specific location and year, the analysis used to assess rainband initiation and withdrawal is based both on the criteria developed above and rainband climatology. The 1982 daily time series for Beijing (Fig. 7) is presented below to illustrate the application of this scheme.

The method focuses on a 90-day period centered on the mean climatological daily precipitation maximum for the 4° zonal band within which the station is located. Figure 4 clearly shows the poleward advance of the monsoon rainband, as indicated by the peak value in each band. Beijing (39°56′N, 116°18′E) is positioned

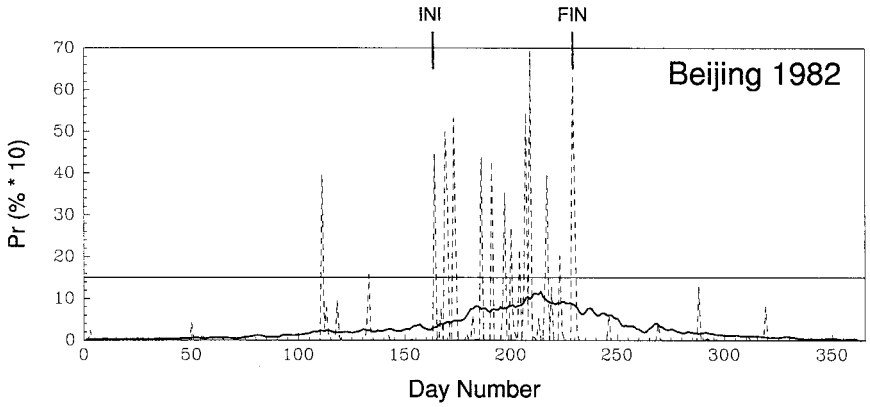

FIG. 7. The 1951–90 mean daily rainfall time series for Beijing (39°56′N, 116°17′E; solid curve) and the 1982 profile (dashed curve). The Pr values (ordinate) are given as a percentage of the annual mean total times 10, where the Pr = 15 line corresponds to the 1.5% heavy rainfall threshold. INI and FIN along the upper *x* axis indicate the rainband initial and final dates, respectively.

within the 36°–40°N band, which has its maximum on day 210 (29 July). Thus, the 90-day period for all stations situated between 36° and 40°N begins on day 165 and ends on day 255. The 25-day running window is initially applied to this 90-day segment of the annual time series to find that period with the maximum number of days when daily rainfall exceeds 1.5%, that is, the ''25-day core period'' of most persistent rainband precipitation. In the case of Beijing in 1982, the 25-day core period is 185–209 and the heavy rainfall threshold is exceeded seven times. From this core period, the 25-day window is moved backward in time until the first window with fewer than 6 heavy rainfall days is encountered. This ''transition window'' defines the 25-day period when rainband precipitation criteria are minimally satisfied and is further examined to determine rainband initiation. To quantify the initial date, the daily time series is analyzed backward in time from the first heavy rainfall day in the transition window until a minimum 5-day period with no measured precipitation is located. The exact initial rainband date is then defined to be the first day following this dry period. For the Beijing 1982 case, the transition window extends from days 180 to 204, the first heavy rainfall day in the window occurs on day 186 and the dry period extends from days 154 to 163. Thus, the initial rainband day is 164 (13 June). Similarly, to ascertain the final rainband date, the running window is moved forward in time from the 25-day core period until a window with fewer then 6 heavy rainfall days is identified. It is from this second transition window that rainband withdrawal is determined. To establish the final date, the daily series is analyzed forward in time from the last heavy rainfall day in the transition window until, again, a minimum 5-day period with no measured precipitation is identified. The precise final rainband date is then defined as the last day with measurable precipitation preceding the dry period. For Beijing in 1982, the second transition window extends from day 209 to 233, the last heavy rainfall day in the window is 231, and the dry period occurs from days 232 to 244. Thus, the final rainband day is 231 (19 August). Note that rain-free periods located within windows where the rainband criteria are satisfied are, regardless of length, identified as break periods. In addition, it is common for persistent rainfall to occur during the days that immediately precede and/or follow transition windows. This is particularly true for south China and the Yangtze River valley. Thus, as is the case with Beijing in 1982, the dry period that signals rainband initiation is identified prior to the first transition window.

Note that rainband duration over Beijing in 1982 is anomalously long (68 days). In addition, there are breaks during this time when little or no rainfall occurs over periods that exceed 5 days. This is a rainband characteristic that is common to all locations throughout China. Thus, application of the 25-day running window ensures that these break periods will not be identified with rainband initiation or withdrawal unless there is a coincident cessation of heavy persistent rainfall.

4. Monsoon characteristics and the Eurasian circulation

The 1951–90 mean initial and final dates are mapped in Figs. 8a,b, which indicate that both attributes increase with latitude. Specifically, the initial monsoon rainband date in south China (20°–27.5°N) is day 138 (18 May). The final date over south China, day 175 (24 June), is found to be several days after rainband initiation over the Yangtze River valley (27.5°–35°N; 12 June). In spite of the fact that the analysis successfully filters tropical precipitation from that attributed to the rainband over south China, overlap occurs because rainband withdrawal over south China is often accompanied by an extended period of light precipitation that coincides with the onset of rainband precipitation over the Yangtze River valley (Fig. 4). In contrast, the Yangtze River

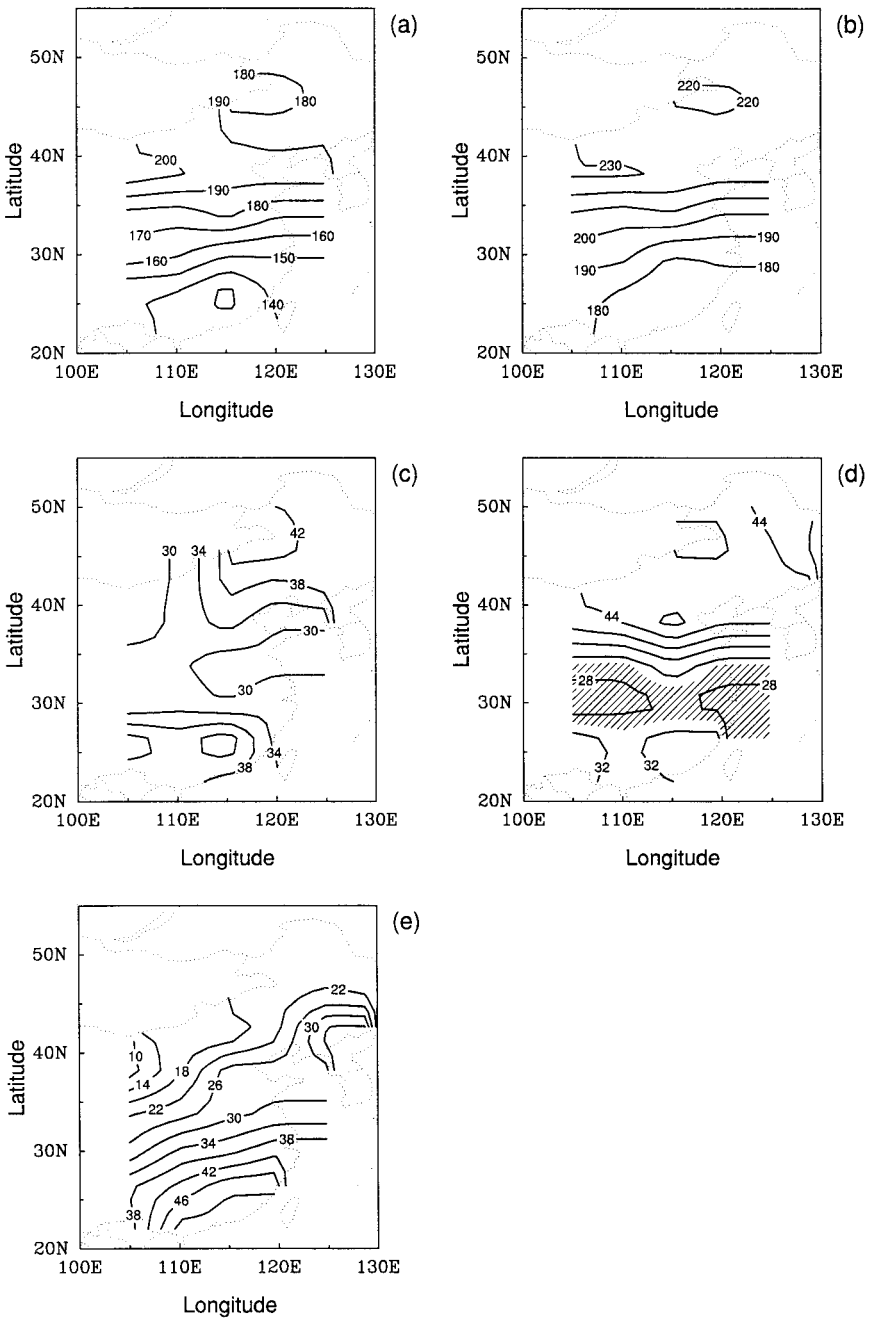

FIG. 8. The 1951–90 mean rainband (a) initial dates (day number), (b) final dates (day number), (c) duration (days), (d) total precipitation (% annual mean) and (e) precipitation amount (cm). The contour intervals are (a)–(b) 10 days, (c) 4 days, (d) 4%, and (e) 4 cm.

valley final date, day 193 (12 July), is nearly the same as the north China (35°–45°N) initial date (10 July) and indicates a more sudden cessation of central China rainfall. The final date over north China is day 224 (12 August). Taken together, Figs. 8a,b provide a general picture of the annual march of the summer monsoon rainband across China. Precipitation typically arrives in south China in mid-May and persists for approximately one month. During the middle of June, the rainband advances from south China to the Yangtze River valley. Then, in mid-July, rainband precipitation ends in the Yangtze River valley and shifts to north China, where it remains until the middle of August. The above results are consistent with those detailed in many studies (e.g., Tao and Chen 1987; Lau et al. 1988; Ding 1992, 1994) and confirm that the method developed in the previous section identifies basic monsoon characteristics, as given by the initial and final rainband dates across China.

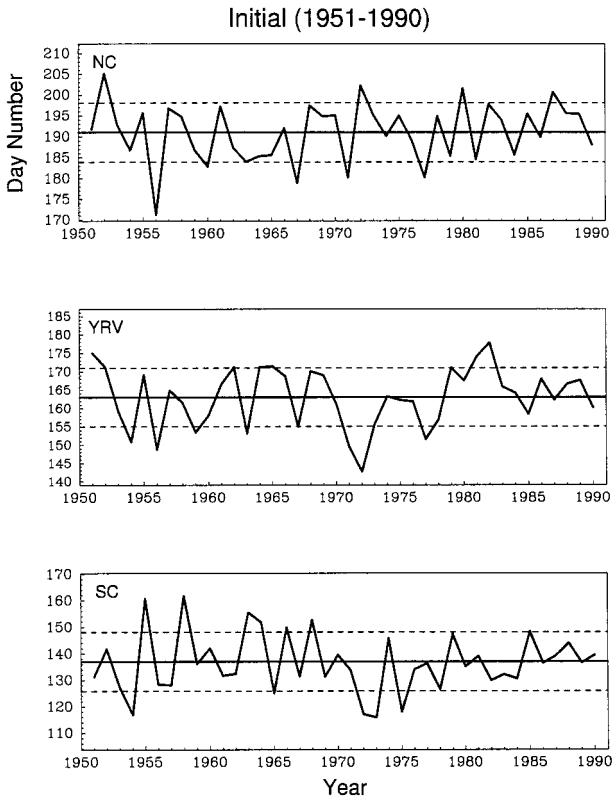

FIG. 9. Monsoon initial date profiles for north China (NC), the Yangtze River valley (YRV), and south China (SC) during the period 1951–90. For each region, the solid horizontal line corresponds to the mean date while the dashed lines indicate values that are one standard deviation above and below the mean.

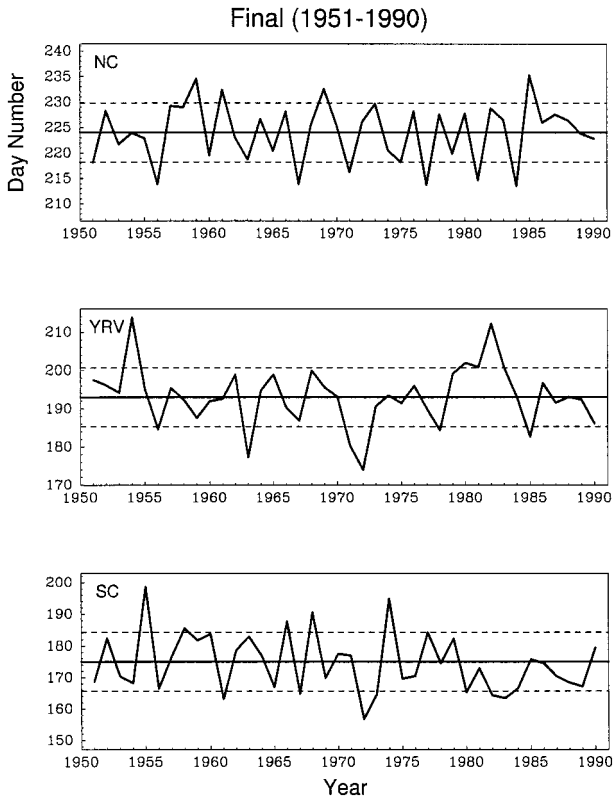

FIG. 10. Same as Fig. 9, except for monsoon final dates.

The initial and final date results are then used to quantify and analyze two additional regional monsoon rainband characteristics. The first is duration (in days), which is the final date minus initial date plus one. The second is total rainfall, which is given as a percentage of mean annual precipitation. The rainband duration field (Fig. 8c) shows maxima over north and south China (34 and 39 days, respectively) and a distinct minimum in the Yangtze River valley (31 days). This indicates that the Yangtze River valley rainband period acts as a transition between periods to the north and south and underscores the results of other studies that show the primary modes of summer rainfall interannual variability to be zonally aligned and centered over the three regions (e.g., Samel et al. 1995; Nitta and Hu 1996). Total rainband precipitation (Fig. 8d) is 31% over south China, decreases to 29% over the Yangtze River valley, and then increases sharply to 43% over north China. As is the case with duration, values are zonally aligned, where the Yangtze River valley is a transition zone between the north and south. On the other hand, actual rainfall amount (Fig. 8e) decreases smoothly from southeast to northwest with a maximum of 50 cm along the south coast and a minimum of less than 10 cm in the north-central interior. Note that, for the remainder of this study, total rainfall is given as a percentage of mean annual precipitation.

In order to examine rainband interannual variability, station values are averaged to produce 1951–90 regional time series for the above characteristics over south China (20°–27.5°N), the Yangtze River valley (27.5°–35°N), and north China (35°–45°N). The choice of these regions is supported by the results shown in Fig. 8. Earlier observational and GCM studies have also shown summer rainfall interannual variability to be focused over the same areas (e.g., Samel et al. 1995; Liang et al. 1994; Nitta and Hu 1996).

The 1951–90 initial and final date time series (Figs. 9 and 10, respectively) reveal large interannual variability throughout China, where regional correlations between the two rainband characteristics are positive and statistically significant at the 99% level (Tables 1–

TABLE 1. Correlation matrix for 1951–90 monsoon rainband initial dates (I), final dates (F), duration (D), and total rainfall (R) over south China. Coefficient magnitudes greater than 0.31 (0.45) are statistically significant at the 95% (99%) level.

	I	F	D	R
I	+1.00	+0.75	−0.57	−0.39
F		+1.00	+0.13	+0.25
D			+1.00	+0.84
R				+1.00

TABLE 2. Same as Table 1, except for the Yangtze River valley. Values in parentheses are correlations following the removal of 1954 from the time series.

	I	F	D	R
I	+1.00 (+1.00)	+0.65 (+0.85)	−0.46 (−0.45)	−0.24 (−0.08)
F		+1.00 (+1.00)	+0.38 (+0.08)	+0.50 (+0.29)
D			+1.00 (+1.00)	+0.93 (+0.71)
R				+1.00 (+1.00)

3). This indicates that rainband duration over each region is relatively stable, where early (late) initiation is followed by early (late) withdrawal. In addition, a strong quasi-biennial oscillation signal is identified over south and north China while variations over the Yangtze River valley generally have longer periodicities.

The regional time series for duration (Fig. 11) show substantial interannual variability, where the most extreme values occur over the Yangtze River valley and range from 22 days in 1966 to 64 days during 1954. Correlations between initial dates and duration (Tables 1–3) are negative and significant at the 99% level for each region, such that early (late) rainband initiation corresponds to increased (decreased) duration. The correlation between final date and duration is positive over each region but significant only for the Yangtze River valley (Table 2; $r = +0.38$), where early (late) rainband withdrawal is identified with decreased (increased) duration. This last result is strongly influenced by 1954 duration, which is 4.9 standard deviations above the mean. The correlation after 1954 is removed from the time series is only +0.08 and much more in line with values for north and south China. Figure 11 also reveals decadal variability in the duration time series over each region. These variations appear to result from low-frequency oscillations in the initial and/or final date time series (Figs. 9 and 10) and will be described below in greater detail. Finally, note that the largest deviations from mean duration occur when the corresponding initial and final date anomalies are strongly out of phase, for example, the Yangtze River valley in 1954.

Total rainband precipitation interannual variability is large over all three regions (Fig. 12), where extreme values range from 19% in the Yangtze River valley during 1985 to 66% over north China in 1959. Correlations between total rainfall and duration (Tables 1–3) are significantly greater than zero at the 99.9% level and reveal the most dominant relationship between rainband characteristics, where increased (decreased) precipitation corresponds to a longer (shorter) rainband period length. Given this association, substantial total rainfall decadal variability is identified over each region, where values are anomalously heavy (light) over north China during 1956–67 (1968–90), the Yangtze River valley during 1953–58 (1959–66 and 1984–90), and south China in 1971–78 (1979–90). The negative values over north China support the results of Wang and Li (1990), Chen et al. (1992) and Yatagai and Yasunari (1994, 1995), who identified persistent negative rainfall anomalies across this region during the 1970s and 1980s. The literature, however, contains little discussion of low-frequency rainfall oscillations over the Yangtze River valley and south China. Also note that correlations between total rainfall and initial dates are significantly less than zero over north and south China (−0.39 and −0.50, respectively), while the positive relationship between total rainfall and final dates is significant only over the Yangtze River valley (+0.50). When 1954 is removed from the Yangtze River valley time series, however, this final correlation is no longer significant (+0.29). These values are consistent with the correlations identified between rainband duration and the initial and final dates. Finally, the total rainband precipitation results clearly show the Yangtze River valley floods of 1954 and 1983 (Huang and Wang 1985; Chen et al. 1992; Nitta and Hu 1996).

Unfortunately, with the exception of extreme events, there are virtually no monsoon rainband characteristics cited in the literature that can be used as a basis for comparison with the above results. However, subjectively determined rainband initial and final dates, duration, and total precipitation (measured) have been made available for the Yangtze River valley by the Beijing Meteorological Center (Chen at al. 1992). These values represent averages for five stations located immediately along the Yangtze River and are used to construct a 1951–90 time series for each rainband characteristic (note that data for only three of these stations are available for the current study). The subjective time series are then correlated with the corresponding series provided by the above analysis (i.e., Figs. 9–12). Initial and final date, duration and total rainfall coefficient values are +0.42, +0.57, +0.44, and +0.73, respectively. Each correlation is significant at the 95% level while the final date and total rainfall coefficients are significant at the 99% level. These results confirm that the analysis developed in this study is able to reproduce subjectively determined rainband characteristics over the Yangtze River valley.

TABLE 3. Same as Table 1, except for north China.

	I	F	D	R
I	+1.00	+0.67	−0.59	−0.50
F		+1.00	+0.20	+0.11
D			+1.00	+0.89
R				+1.00

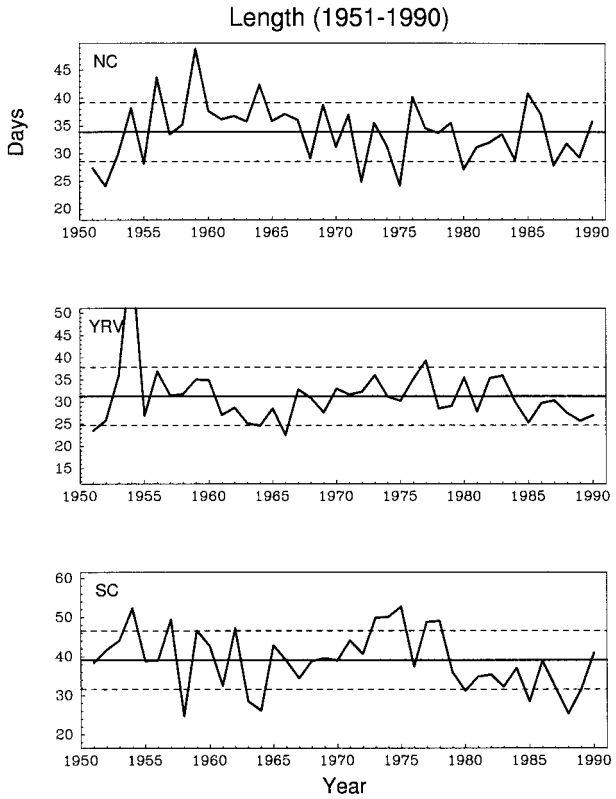

FIG. 11. Same as Fig. 9, except for monsoon duration, in days.

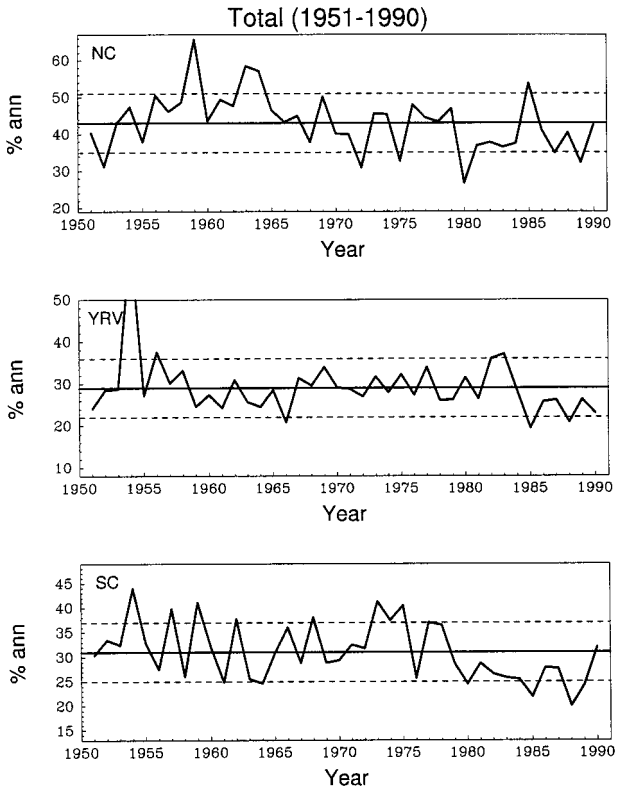

FIG. 12. Same as Fig. 9, except for total monsoon rainfall, in percent of mean annual total.

5. Relationships with the Eurasian circulation

Given that the study methodology generates realistic rainband initial and final date, duration, and total precipitation values that have substantial interannual variability, relationships with Eurasian circulation features are next identified. It has been shown in previous research that summer rainfall interannual variability over China is linked to variations in the configuration of the Eurasian circulation pattern. Murakami and Matsumoto (1994) determined that rainfall along the Mei-Yu front is related to the strength and location of both the subtropical and monsoon highs. Wang and Zhang (1992) correlated sea level pressure with dryness indices for north China, the Yangtze River valley, and south China and found a link with the position of the subtropical high. Yatagai and Yasunari (1994, 1995) performed EOF analysis on the summer rainfall field over East Asia and then correlated the temporal coefficients with Eurasian sea level pressure and 500-hPa-height fields. Results indicate a significant correlation between westward expansion of the subtropical high and increased rainfall over the Yangtze River valley and north China. Similarly, Nitta and Hu (1996) correlated EOF temporal coefficients with the Eurasian circulation and found a comparable set of results for Yangtze River valley summer rainfall. Samel at al. (1995) correlated Eurasian sea level pressure and 500-hPa height fields with summer rainfall intensity indices for the Yangtze River valley and southeast China and found that interannual variability is explained by interactions between several features, including the monsoon low, Siberian high, and subtropical high.

In the studies listed above, no distinction was drawn between summer rainfall and precipitation attributed specifically to the monsoon rainband. Hence, in this investigation, statistically significant relationships are identified between the Eurasian circulation and total rainband precipitation interannual variability over north China, the Yangtze River valley, and south China. Single point correlations are calculated between total rainfall anomalies (in percent of annual mean total) over each region and gridded Eurasian sea level pressure and 500-hPa-height anomalies for the period 1951–90. Coefficient values are mapped and analyzed, where correlations are statistically significant at the 95% level when the coefficient magnitude is greater than 0.31. Total rainfall is chosen for this analysis because heavy persistent precipitation is the primary physical manifestation of the monsoon rainband.

For each region in China, the correlations are performed over two consecutive months. The rationale for this approach is simple. Although average rainband duration is approximately one month over each region, the actual period typically straddles two months. The

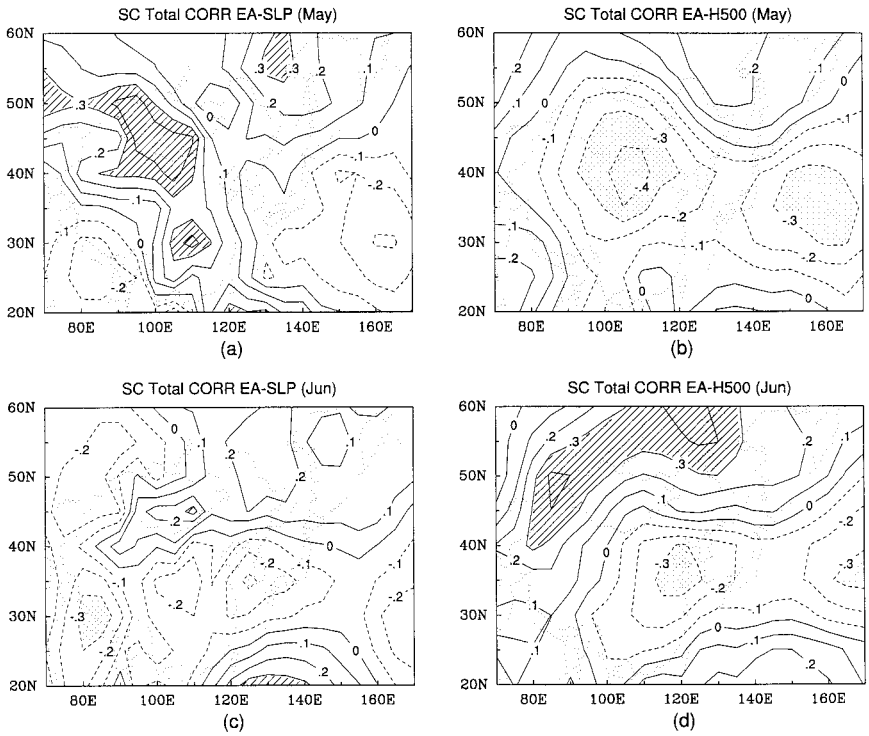

FIG. 13. Correlations between SC total rainfall and the (a) May, (c) June Eurasian sea level pressure and (b) May, (d) June 500-hPa-height fields. The contour interval is 0.1. Positive (negative) values with a magnitude greater than 0.31 are significant at the 95% level and are hatched (stippled).

months chosen for each region correspond to those during which the mean initial and final rainband dates occur. For south China, the Yangtze River valley, and north China, the two months are May–June, June–July, and July–August, respectively. Note that all relationships below are discussed in terms of increasing precipitation.

Significant positive correlations between south China total rainband precipitation and Eurasian sea level pressure in May are identified over several areas (Fig. 13a). The primary centers occur along an axis that extends from central Siberia to the South China Sea. The correlation pattern links increased precipitation with southward ridging of the Siberian high, which causes both the longitudinal pressure gradient and cold air advection to increase over south China. When total rainfall is correlated with May 500-hPa heights (Fig. 13b), two significant negative centers are found along an east–west axis at approximately 40°N. The primary area is over north China and indicates a baroclinic response in the height field associated with the southward extension of the Siberian high. The resulting 500-hPa height pattern produces anomalous southwesterly flow and moisture advection over south China. Taken together, Figs. 13a,b provide a physically consistent picture, where increased south China total rainfall occurs in conjunction with the intrusion of cold air at lower levels and overrunning by warm moist air aloft. This scenario closely resembles that outlined by Ding (1992) and Chen and Chen (1995).

During June (Figs. 13c,d), there are substantial changes in the correlation fields and, as a result, the circulation features that explain total rainfall variations over south China. The pattern is nearly barotropic, with positive centers over north Asia and the south China coast. Significant negative correlations are located along an axis that extends from the Indian subcontinent (sea level pressure only) to the west-central Pacific Ocean between 35° and 40°N. The coefficient pattern indicates increased (decreased) heights over southern Siberia (northeast China) and westward ridging of the subtropical high toward south China. The resulting fields produce an increased pressure gradient as well as enhanced southwest flow and moisture transport over south China.

The correlation between Yangtze River valley total rainfall and the Eurasian sea level pressure field for June (Fig. 14a) produces a positive center over north-central China and negative areas along an axis from India to the Yangtze River valley. The pattern identifies increased Yangtze River valley total rainfall with changes in the Siberian high, Mei-Yu front, and the monsoon low. As each feature intensifies, the resulting circulation pattern causes convergence, the thermal gradient, and upward motion to increase along the Mei-Yu front.

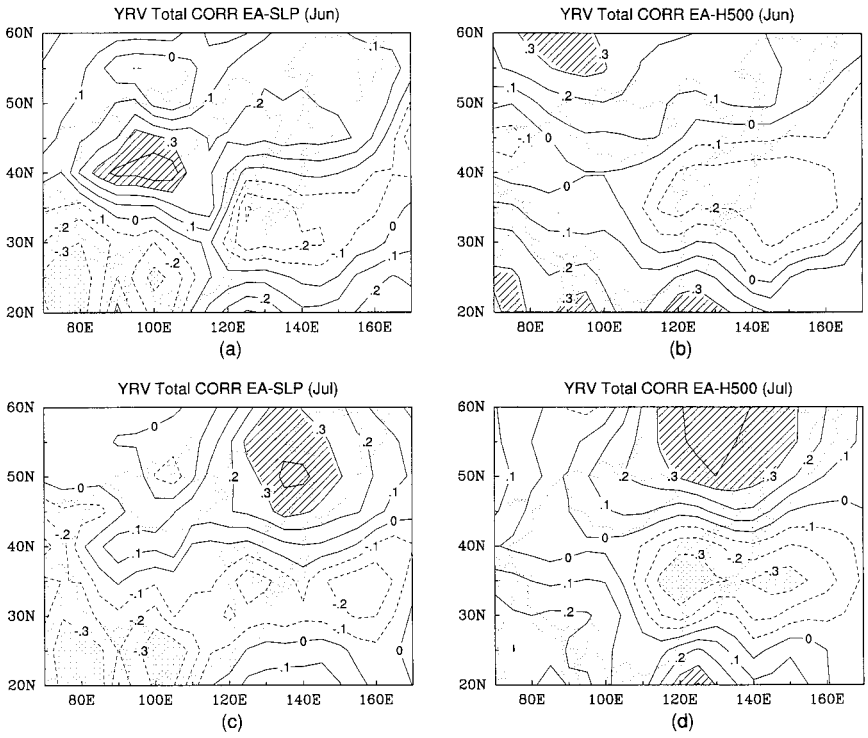

FIG. 14. Same as Fig. 13, except that correlations are calculated between YRV total rainfall and the (a) June, (c) July Eurasian sea level pressure and (b) June, (d) July 500-hPa-height fields.

Anomalous southwesterly flow along the east side of the monsoon low also enhances moisture transport over the Yangtze River valley. Significant positive correlations between total rainband precipitation and June 500-hPa heights (Fig 14b) extend from India to the west Pacific Ocean. The Pacific Ocean center signals a southwest shift of the subtropical high while the positive areas over south Asia correspond to an intensification of the monsoon high. These features act to enhance southwest flow and moisture advection over south China as well as confluence along the Yangtze River valley. Taken together, Figs. 14a,b indicate that heavy Yangtze River valley rainband precipitation is identified with an intensified Mei-Yu front and deep upward vertical motion during June. This description agrees with those of Chen and Chang (1980) and Ding (1992), who discussed a vertical axis of strong ascending motion that closely corresponds to Mei-Yu front location.

It is important to note that meaningful differences exist in the June sea level pressure features that explain increased total rainband precipitation over south China (Fig. 13c) and the Yangtze River valley (Fig. 14a). The correlation fields for both regions clearly show a trough that extends from south Asia to the east China coast. Relative to the Yangtze River valley, however, the trough axis in the south China case is displaced poleward by approximately 5° and corresponds to ridging of the subtropical high toward the southeast coast. This feature generates anomalous southwest flow and moisture transport over south China during years with heavy rainband precipitation. In addition to the trough axis, both the south China and Yangtze River valley cases show the Siberian high ridging over southern Mongolia and north central China. Intensification of this feature, however, is much greater in the Yangtze River valley case. This leads to the advection of cold air over the region which, in turn, focuses baroclinicity, convergence, and upward motion along the Mei-Yu front.

Although the correlation patterns between Yangtze River valley total rainfall and the July Eurasian circulation (Figs. 14c,d) are similar to those for June, there exist meaningful differences. Significant positive correlations between total rainfall and sea level pressure in July (Fig. 14c) are found over east Siberia–Sea of Okhotsk. It has been shown that a blocking high over the Sea of Okhotsk becomes established when heavy rainfall occurs along the Yangtze River valley (Tao and Chen 1987; Samel et al. 1995; Liang and Wang 1997, manuscript submitted to *Quart. J. Roy. Meteor. Soc.*), where transient disturbances on the south side of the high advect cold air over the Yangtze River valley and sharpen the thermal gradient along the Mei-Yu front. The correlation pattern between total rainfall and the July 500-hPa-height field (Fig. 14d) contains two significant positive centers over east Siberia–Sea of Okhotsk and the south China coast. An elongated area of negative coefficients extends along 35°N from east China to the west Pacific Ocean. The coefficient pattern

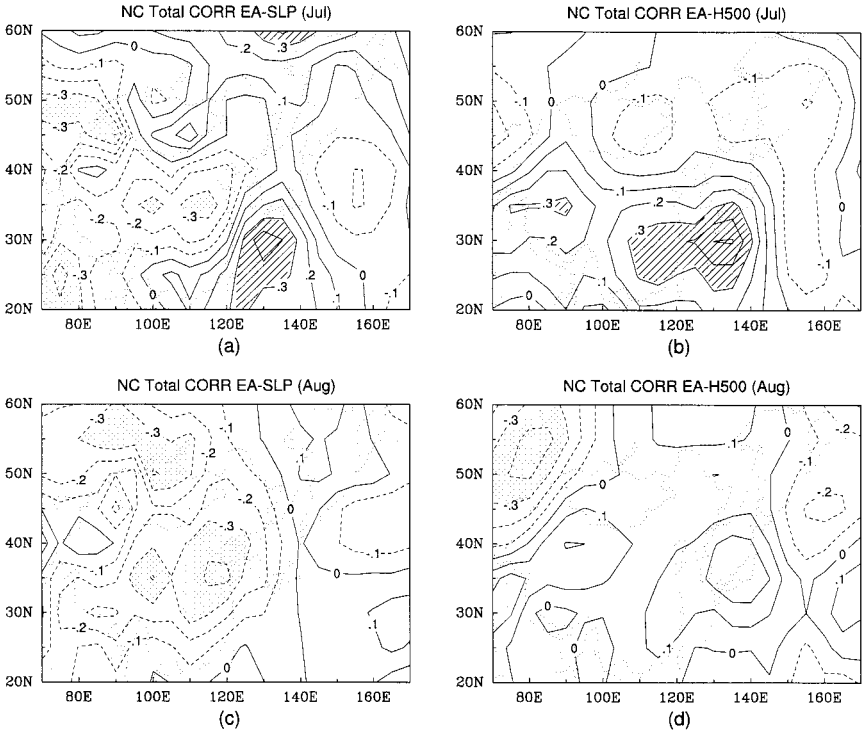

FIG. 15. Same as Fig. 13, except that correlations are calculated between NC total rainfall and the (a) July, (c) August Eurasian sea level pressure and (b) July, (d) August 500-hPa-height fields.

indicates that total rainfall increases correspond to an intensification of the Okhotsk high, lower heights along 35°N, and ridging of the subtropical high toward the southeast China coast. The enhanced gradient between the midlatitude trough and subtropical high produces anomalous southwest flow and moisture transport across the Yangtze River valley.

The correlation pattern between north China total rainfall and July sea level pressure (Fig. 15a) shows significant negative centers that extend from India to northeast China and large positive values along the east China coast. This indicates that north China total rainfall increases occur in conjunction with lower pressures over east China and westward ridging of the subtropical high. The resulting longitudinal pressure gradient increase along the east China coast causes moist south to southeast flow to strengthen over north China. Cao (1990) found that westward ridging of the subtropical high plays a dual role by enhancing moisture advection over the region while blocking the eastward advance of upstream troughs. Significant positive correlations between total rainfall and July 500-hPa heights (Fig. 15b) are located along 30°–35°N and extend across China to the west Pacific Ocean. Placement of the Pacific Ocean center is consistent with the barotropic nature of the subtropical high while that over east China is explained by latent heat release over the landmass that results from convection. Taken together, Figs. 15a,b indicate that north China total rainband precipitation increases in response to reduced east China surface pressures, westward ridging of the subtropical high, and enhanced low-level moisture transport over the region.

Note that there are substantial differences in the July circulation features that explain increased total rainband precipitation over the Yangtze River valley and north China. While the sea level pressure correlation fields for both regions (Figs. 14c and 15a) clearly show lower values that extend from south Asia to the east China coast, the trough axis in the north China case (Fig. 15a) is displaced poleward approximately 5°. This result corresponds closely with Tao and Chen (1987), who identified rainband movement from the Yangtze River valley to north China with a poleward jump in the position of the subtropical high. Also apparent during the north China case is ridging of the subtropical high along the east China coast. Both features interact to generate anomalous south to southeast flow and moisture transport over north China. Conversely, the Okhotsk high, which has been related to Mei-Yu front intensification, is identified only during the Yangtze River valley case (Fig. 14c). The 500-hPa-height correlation field for the north China case (Fig. 15b) indicates a baroclinic response over the landmass associated with latent heat release and a barotropic reflection of the Pacific Ocean subtropical high. The Yangtze River valley pattern (Fig. 14d), on the other hand, is essentially barotropic throughout Eurasia. Finally, 500-hPa subtropical high ridging in the north China case occurs approximately

10° farther north than that for the Yangtze River valley case. This is consistent with the results of Tao and Chen (1987), who found that the poleward extent of monsoon rainfall increases as the subtropical high over the west-central Pacific Ocean moves farther to the north.

The correlation pattern between north China total rainfall and August sea level pressure (Fig. 15c) is similar to that for July, where significant negative values are located along an axis that extends from India to the north China coast. Areal coverage, however, is much greater in August. This indicates that increased north China rainband precipitation occurs in conjunction with decreased sea level pressures over east China, which produce enhanced south to southeast flow and moisture advection over north China. Correlations between August 500-hPa heights and total rainfall (Fig. 15d) are comparable to those for July, but there is a complete absence of significant coefficients over the monsoon region.

To verify the above correlations, monthly sea level pressure and 500-hPa-height anomaly composites are calculated for sets of years when south China, Yangtze River valley, and north China total rainband precipitation anomaly magnitudes are greater than one standard deviation above the mean (Fig. 12). For both fields, the difference between the positive and negative composites is computed and mapped. The results (not shown) indicate that the largest anomaly center locations correspond very closely to the correlation centers shown in Figs. 13–15, where all spatial correlations between the correlation and composite sea level pressure and 500-hPa-height maps are statistically significant at the 99% level.

Finally, it is very important to note that the correlation analysis results described above indicate substantial changes in the monthly Eurasian circulation features that explain regional total rainband precipitation interannual variability. This differs from earlier studies, where monsoon precipitation is defined to occur over a fixed period of several months. For example, Samel et al. (1995) correlated summer (June, July, August) Yangtze River valley rainfall with the Eurasian sea level pressure field. The resulting coefficient pattern was composed of the dominant circulation features found during both June and July (Figs. 14a,c). This indicates that the semiobjective analysis developed in section 3 allows us to better resolve relationships that exist between rainband precipitation and various Eurasian circulation features during different phases of the rainband period.

6. Summary

In previous observational and modeling studies of the East Asian summer monsoon rainband, the assumption of a multiple-month fixed-period length has precluded an investigation of initial and final date interannual variability. The inability to objectively determine these characteristics has made it difficult to identify relationships that exist between rainband precipitation and the larger Eurasian circulation due to the mixing of atmospheric mechanisms that have smaller-scale temporal variations. Hence, this observational study had two objectives. The first was to quantify observed monsoon rainband interannual variability across China. The second was to ascertain associations between total monsoon rainband precipitation and the Eurasian circulation. The analyses utilized in this research were developed to facilitate the future comparison of observed rainband characteristics with GCM simulations.

Normalized 1951–90 daily rainfall for 85 observation stations were used in this study where, for each location, values were given as a percentage of the annual mean total. The annual time series were analyzed to develop a rainband precipitation definition based on the occurrence of heavy, persistent rainfall. CFDs based on daily amount were first produced for 4° zonal bands and an approximate 90% statistical threshold was applied to define a ''heavy'' rainfall day as one when precipitation exceeds 1.5% of the mean annual total. A 25-day moving window was then applied to all yearly time series between the first and last days when rainfall exceeded 1.5%. CFDs based on the total number of heavy rainfall days in each window showed that 90% of the windows have 6 or less days when rainfall exceeds 1.5%. As a result, heavy precipitation was defined to be persistent and thus, identified with the rainband, when the 1.5% threshold is exceeded six or more times in a 25-day period. Finally, frequency distributions of the consecutive number of days with zero and nonzero precipitation indicated that the hydrologic cycle over China rarely remains active or dormant for a period that exceeds 5 days. Hence, a minimum of 5 consecutive days with no measurable rainfall was chosen as the requirement used to identify the initiation and withdrawal of rainband precipitation at a specific location. The semiobjective analysis used to identify annual initial and final rainband dates at each location was based on the above definitions and the daily precipitation climatology for the zonal band within which the station is located.

Initial and final rainband dates were analyzed for three broad regions: south China, the Yangtze River valley, and north China. Results indicate that the approach developed above identifies rainband movement that closely corresponds to the systematic poleward advance of summer monsoon precipitation across China (e.g., Tao and Chen 1987; Lau et al. 1988; Ding 1992, 1994). Average rainband duration was found to be approximately 30–40 days while total rainfall decreases from south to north. A statistically significant positive relationship was identified between duration and total rainfall interannual variability over each region. In particular, both characteristics decreased substantially over north China after 1967. This result is consistent with Wang and Li (1990), Chen et al. (1992), and Yatagai and Yasunari (1994, 1995), who identified increased de-

sertification over this region during the 1970s and 1980s.

Correlation analysis was then used to quantify statistically significant relationships between total rainfall over each region and the Eurasian sea level pressure and 500-hPa-height fields. The coefficient patterns indicate that rainfall mount is influenced by the interaction of several circulation features. Precipitation over south China was found to increase when low-level cold air identified with southward ridging of the surface Siberian high becomes established over east China and is overrun by a southwest flow of warm moist air. Yangtze River valley rainfall is enhanced when the subtropical high ridges toward the east China coast and both the Siberian high and monsoon low strengthen. This causes moisture transport, upward motion, and the thermal gradient to intensify along the Mei-Yu front. In addition, higher pressures were identified over the Sea of Okhotsk, where the development of an Okhotsk high has been shown to sharpen the Mei-Yu front temperature gradient (e.g., Tao and Chen 1987). Total rainband precipitation over north China was found to increase in response to intense heating over the Eurasian landmass, ridging of the subtropical high along the east China coast, and enhanced moisture advection that results from increased south to southeast flow over the region. The results of the correlation analysis indicate substantial changes in the Eurasian circulation features that explain total rainfall interannual variability during the rainband period. This differs from earlier studies, where monsoon precipitation is defined to occur over a fixed period of several months and the results show a mixture of the dominant circulation features described above (i.e., Samel et al. 1995).

The results of this observational research indicate the existence of statistically significant and physically relevant relationships between rainband precipitation over China and the larger Eurasian circulation. The analysis used to identify rainband initiation and withdrawal was designed such that an identical analysis can be performed with model simulations. Hence, in the follow-up to this investigation, the ability of a GCM to reproduce observed east Asian summer monsoon rainband characteristics over north China, the Yangtze River valley, and south China will be determined. A very careful analysis of the simulated daily rainfall data will be required because discrepancies are expected between the observed and simulated rainband climatologies (Liang and Wang 1997). As a result, differences between observed and GCM definitions for heavy, persistent precipitation and the dry period length required to quantify annual rainband initiation and withdrawal are anticipated. These disparities must then be investigated to identify differences in the GCM and observed Eurasian circulation features that explain rainband precipitation.

The capacity to quantify initial and final rainband date interannual variability throughout China will also enable us to perform a detailed observational–GCM investigation of the dynamic mechanisms that explain abrupt rainband movements. Tao and Chen (1987) and Ding (1994) related the poleward advance of the monsoon to seasonal northward movement of the subtropical high. Sudden transitions identified in rainband initiation over the Yangtze River valley were also identified with rapid changes in the dynamic and thermodynamic fields over Asia. Until recently, an observational investigation has been precluded by the coarse temporal resolution of available observed long-term upper-air datasets (i.e., monthly). However, the newly released National Centers for Environmental Prediction reanalysis archives have four observations per day. This will allow for the calculation of daily lead and lagged correlations which will then be used to identify statistically significant sudden changes in the atmospheric circulation that precede and follow observed rapid rainband advancement between adjacent regions.

REFERENCES

Cao, S.-Y., 1990: The observations of the Huanghai Bohai and the Sea of Japan highs and the heavy rain in north China in summer (in Chinese). *Quart. J. Appl. Meteor.*, **1,** 162–168.

Chang, C.-P., and T.-J. G. Chen, 1995: Tropical circulations associated with southwest monsoon onset and westerly surges over the South China Sea. *Mon. Wea. Rev.*, **123,** 3254–3267.

Chen, L.-X., M. Dong, and Y.-N. Shao, 1992: The characteristics of interannual variations on the east Asian monsoon. *J. Meteor. Soc. Japan*, **70,** 397–421.

Chen, T.-C., and J.-M. Chen, 1995: An observational study of the South China Sea monsoon during the 1979 summer: Onset and life cycle. *Mon. Wea. Rev.*, **123,** 2295–2318.

Chen, T.-J. G., and C.-P. Chang, 1980: The structure and vorticity budget of an early summer monsoon trough (Mei-Yu) over southeastern China and Japan. *Mon. Wea. Rev.*, **108,** 942–953.

Ding, Y.-H., 1992: Summer monsoon rainfalls in China. *J. Meteor. Soc. Japan*, **70,** 373–396.

——, 1994: *Monsoons Over China.* Kluwer Academic, 419 pp.

Fan, Z., and R. J. Oglesby, 1996: A 100-yr CCM1 simulation of North China's hydrologic cycle. *J. Climate*, **9,** 189–204.

Huang, J.-Y., and S.-W. Wang, 1985: Investigations of variations of the subtropical high in the western Pacific during historic times. *Climate Change*, **7,** 427–440.

Hulme, M., Z.-C. Zhao, and T. Jiang, 1994: Recent and future climate change in east Asia. *Int. J. Climatol.*, **14,** 637–658.

Jenne, R., 1989: Data availability at NCAR (selected datasets). National Center for Atmospheric Research Tech. Note NCAR TN/IA-111, 45 pp. [Available from NCAR, P.O. Box 3000, Boulder, CO 80307.]

Lau, K.-M., and M.-T. Li, 1984: The monsoon of east Asia and its global associations—A survey. *Bull. Amer. Meteor. Soc.*, **65,** 114–125.

——, and S. Yang, 1996: Seasonal variation, abrupt transition, and intraseasonal variability associated with the Asian summer monsoon in the GLA GCM. *J. Climate*, **9,** 965–985.

——, G. J. Yang, and S. H. Shen, 1988: Seasonal and intraseasonal climatology of summer rainfall over east Asia. *Mon. Wea. Rev.*, **116,** 18–37.

Liang, X.-Z., and W.-C. Wang, 1997: Associations between China monsoon rainfall and tropospheric jets. *Quart. J. Roy. Meteor. Soc.*, in press.

——, A. N. Samel, and W.-C. Wang, 1994: Observed and simulated decadal variability in monsoon rainfall in China. *Climate Dyn.*, **11,** 103–114.

Liu, Y., F. Giorgi, and W. M. Washington, 1994: Simulation of summer

monsoon climate over East Asia with an NCAR regional climate model. *Mon. Wea. Rev.,* **122,** 2331–2348.

Madden, R., and P. Julian, 1972: Description of global scale circulation cells in the tropics with a 40–50 day period. *J. Atmos. Sci.,* **29,** 1109–1123.

Murakami, T., and J. Matsumoto, 1994: Summer monsoon over the Asian continent and western north Pacific. *J. Meteor. Soc. Japan,* **72,** 719–745.

Ninomiya, K., and T. Akiyama, 1992: Multi-scale features of Baiu, the summer monsoon over Japan and east Asia. *J. Meteor. Soc. Japan,* **70,** 467–495.

Nitta, T., and Z.-Z. Hu, 1996: Summer climate variability in China and its association with 500 hPa height and tropical convection. *J. Meteor. Soc. Japan,* **74,** 425–445.

Samel, A. N., S.-W. Wang, and W.-C. Wang, 1995: A comparison between observed and GCM simulated summer monsoon characteristics over China. *J. Climate,* **8,** 1690–1696.

Sperber, K. R., S. Hameed, G. L. Potter, and J. S. Boyle, 1994: Simulation of the northern summer monsoon in the ECMWF model: Sensitivity to horizontal resolution. *Mon. Wea. Rev.,* **122,** 2461–2481.

Tao, S., and L. Chen, 1987: A review of recent research on the east Asia summer monsoon in China. *Monsoon Meteorology,* T. N. Krishnamurti, Ed., Oxford University Press, 60–92.

——, C. Fu, Z. Zeng, and Q-.Y. Zhang, 1991: Two long-term instrumental climate data bases of The Peoples Republic of China. Publication 3747, Environmental Sciences Division, DOE, 83 pp. [Available from Carbon Dioxide Information Analysis Center, Oak Ridge National Laboratory, Oak Ridge, TN 37831-6335.]

Wang, P. K., and D. Zhang, 1992: Recent studies of the reconstruction of east Asian monsoon climate in the past historical literature of China. *J. Meteor. Soc. Japan,* **70,** 423–446.

Wang, W.-C., and K. Li, 1990: Precipitation fluctuation over semiarid region in northern China and the relationship with El Niño/Southern Oscillation. *J. Climate,* **3,** 769–783.

Yatagai, A., and T. Yasunari, 1994: Trends and decadal fluctuations of surface air temperature and precipitation over China and Mongolia during the recent 40-year period (1951–1990). *J. Meteor. Soc. Japan,* **72,** 937–957.

——, and ——, 1995: Interannual variations of summer precipitation in the arid/semi-arid regions in China and Mongolia: Their regionality and relation to the Asian summer monsoon. *J. Meteor. Soc. Japan,* **73,** 909–923.